ISSN 0915-633X

NATIONAL INSTITUTE FOR FUSION SCIENCE

Tunneling Electron Trap

T. Ohkawa

(Received - Nov.7, 1997)

NIFS-524 Dec. 1997

RESEARCH REPORT
NIFS Series

NAGOYA, JAPAN

Tunneling Electron Trap

Tihiro Ohkawa

National Institute for Fusion Science

and

University of California, San Diego

Abstract

The use of the field emission as means of filling the electron traps is proposed. Because of the electron tunneling at the cathode tip, the energy of the emitted electrons is lower than the electrostatic potential of the tip surface by the work function of the tip material. Consequently the electrons are trapped by the electrostatic well without requiring the dynamic trapping. The Brillouin density will be reached readily because the injection on the axis of the cylindrical symmetry dictates that the canonical angular momentum of the electrons vanishes. Furthermore the evaporative cooling due to the electrons escaping from the trap over the potential barrier may be able to cool the trapped electrons to cryogenic temperatures. The interesting regimes of the strongly correlated plasma and the quantum mechanical plasma may be obtained.

Keywords: electron trap, field emission, tunneling effect, cooling of electrons, electron plasma, strongly correlated electron plasma

1. Introduction

The physical behaviors of non-neutral plasma have been studied in various charged particle traps, a typical of which is Penning-Malmberg trap as shown in Fig 1. It is a cylindrical trap where the radial motion of the charged particles are constrained by magnetic field, while the longitudinal motion is constrained by an electrostatic potential well. When used as an electron trap, the electrons from a thermionic cathode are injected parallel to the magnetic field while the cathode side of the electrostatic well is open. By closing the well dynamically, the electrons which fail to escape during the well closure will be trapped. Because of the low current density available from thermionic cathodes, the electron density on the trap is limited to well below the Brillouin limit.

The trapped electron density may be increased greatly by taking advantage of the electron tunneling. Suppose we place a channel through which electrons can tunnel into the electrostatic well. The kinetic energies of the electrons after entering into the well via tunneling is smaller than the height of the potential barrier of the well. Consequently the electrons will bounce around inside the well until they find the channel. The probability of the tunneling back is small [$< 10^{-6}$] and the electrons accumulate during many transit times. Hypothetically a steady state is reached when the electron density in the trap is equal to the electron density at the source. If the source is a metal, the density of the electrons in the conduction band is huge [$> 10^{28}\ m^{-3}$]. Therefore it is likely that the electron density is limited by other physical processes before it reaches the steady state with the source.

Meantime the velocity distribution of the electrons in the trap become Maxwellian due to the electron-electron collisions, the electrons in the Maxwellian tail may have sufficient energies to escape from the trap. The energies of the escaping electrons are always higher than the energy of the electrons tunneling in. Thus the evaporative cooling takes place and the electron temperature decreases.

As the number of the trapped electrons increases the potential energy of the electrons in the trap becomes higher until the tunneling ceases. The evaporative cooling may continue until the electron temperature becomes so low and the evaporation stops.

The field emission cathode can act as the channel described above. The electrons in metal is confined by the potential barrier at the interface between metal and vacuum which is called the work function. When a strong electric field perpendicular to metal surface is applied the thickness of the potential barrier is reduced and the electrons can tunnel out into vacuum resulting in the field emission.

In the following the characteristics of the field emission, the equilibrium of the electron plasma, the filling of the trap by the field emission cathode, the evaporative cooling, the collisional heating, the field error effects and the attainable plasma regimes will be discussed.

2. Field Emission

A simplified energy diagram of the electrons at metal vacuum interface is shown in Fig-2. A negative voltage V is applied to the metal with respect to vacuum. The metal electrons are in the conduction band and the energy difference between the surface and the bottom of the conduction band is the work function $e\phi$. Typically ϕ is 4~5 volts. At a finite temperature T the electrons are distributed kT above the bottom of the conduction band. When the applied electric field is large and the thickness of the potential barrier is reduced, the electrons will tunnel out to vacuum. The energy W of the tunneled out electrons in vacuum is given by

$$W = -eV - e\phi + 2kT \tag{1}$$

Because a very high electric field [$> 10^9$ V/m] is required for a significant emission current, the cathode is usually shaped as a sharp needle. The perpendicular electric field at the surface of the tip is approximately given by

$$E = [-V + \Phi_0] / R \tag{2}$$

where R is the radius of the curvature of the tip and Φ_0 is the potential of the anode. The thickness of the barrier increase with R and the tunneling is concentrated near the very tip.

The field emission current density is given by Fowler-Nordheim formula [1].

$$j = \alpha E^2 exp\,(-\beta/E) \tag{3}$$

where j is the current density in A/m^2, E is the electric field strength in V/m, ϕ is the work function in volt and

$$\alpha = 1.5 \times 10^{-6} \phi^{-1} exp\,(10.4\,\phi^{-1/2}) \tag{4}$$

$$\beta = 6.44 \times 10^9\,\phi^{3/2} \tag{5}$$

An example set of numbers is $\phi = 4$ volt, $E = 5 \times 10^9$ V/m and $j = 10^{10} A / m^2$.

By assuming that the emitting area is R^2 the current I from the tip is given by

$$I = \alpha\,(V')^2 exp\,(-\beta R / V') \tag{6}$$

where $V' = -V + \Phi_0$.

With a very sharp tip, i.e.,. a very small R, the high electric field necessary for a sufficient field emission current may be obtained at a relatively low voltage . When the voltage V' becomes comparable to the work function ϕ, the above formula which assumes $V' >> \phi$ must be modified because the potential barrier against the tunneling becomes wider than the formula indicates.

We assume that the tip is a sphere of the radius R and estimate the tunneling probability. The revised formula becomes,

$$I = \alpha\,(V')^2 exp\left[-(\beta R/V')\left\{-2V'/\phi - 2ln(1-\phi/V')(V')^2\phi^{-2}\right\}\right] \tag{7}$$

where the anode is assumed be at infinite. At the limit of $V' >> \phi$ the formula become identical to eq(6). At around $V'=2\phi$ a noticeable reduction of the current occurs and at $V'= 1.5\,\phi$ the current is severely reduced.

The I-V' characteristics of a cathode tip can be measured experimentally. The parameters α and βR are determined from the measured characteristics. It is expected that they vary from tip to tip.

Since the invention of the micro-cathode tips by C.A. Spindt [2] the field emission array [FEA] has been under development for vacuum micro-electronics applications. One of the development effort is to reduce the operating voltage. The life time of the cathode tips depends on the degradation due to the sputtering by the ions of the residual gas atoms or molecules accelerated toward the tip. By lowering the operating voltage the ion energy can be below the sputtering threshold [~30eV]. Better yet if the operating voltage is below the ionization energy the ions will be absent. The cathodes workable below 10 volts are being developed.

In parallel the scanning tunneling electron microscope has become practical. The probe tips are required to have small R for this application also. The resolution of atomic dimension has been obtained when a small bump of atomic scale is emitting electrons.

3. Electron Plasma Equilibria

In a cylindrical trap where the effect of the field errors and the collisions with the residual gas can be neglected, the energy of the electron H and the canonical angular momentum p_θ are constants of the motion. The Boltzmann distribution has the form [3]

$$f = n_0(m/2\pi kT_e)^{3/2} exp\,[-(H - \omega p_\theta)/kT_e] \tag{8}$$

where

$$H = mv^2/2 - e\Phi$$

$$p = mv_\theta r - eBr^2/2$$

m is the electron mass, v is the electron velocity, Φ is the electrostatic potential and B is the magnetic field.

The substitution of H and p_θ in eq (8) yields

$$f = n(m/2\pi kT_e)^{3/2} exp\left[-\left(\vec{v} - \omega r\vec{\theta}\right)^2 m/2kT_e\right] \tag{9}$$

$$n = n_0 exp\left[-\{-e\Phi + m\omega(\Omega - \omega)r^2/2\}/kT_e\right] \tag{10}$$

where Ω is the cyclotron frequency, $\Omega = eB/m$. The velocity distribution is a rotating Maxwellian with angular frequency ω. The total number of the electrons, the total angular momentum and the total energy determine n, T_e and ω.

The plasma potential and the electron density are related through the Poisson's equation

$$\nabla^2\Phi = en/\varepsilon_0 \tag{11}$$

For the cases where the Debye length λ_D is much smaller than plasma radius a, the self consistent density distribution satisfying eq (10) and eq (11) is nearly constant density to the radius a and falls off steeply within about the Debye length. By assuming that the density is constant inside the plasma $0 \le r \le a$ and vanishes between the plasma and the wall $a \le r \le b$, we obtain

$$\begin{aligned} e\Phi &= m\omega(\Omega - \omega)\{r^2/2 - a^2/2 - a^2 ln\,(b/a)\}\ , \quad 0 \le r \le a \\ e\Phi &= m\omega(\Omega - \omega)a^2 ln\,(r/b) \qquad\qquad a \le r \le b \end{aligned} \tag{12}$$

and

$$\begin{aligned} n &= 2\varepsilon_0 m\omega(\Omega - \omega)e^{-2} \qquad 0 \le r \le a \\ n &= 0 \qquad\qquad a \le r \le b \end{aligned} \tag{13}$$

The electrons are injected from cathode with a very small tip placed on the cylindrical

axis, Therefore all electrons have vanishingly small canonical angular momentum and the total canonical momentum must vanish. The condition given by

$$\int dv^3 \int_0^a (mrv_\theta - eBr^2/2) f dr = 0 \tag{14}$$

results in

$$\omega = \Omega / 2 \tag{15}$$

$$n = \varepsilon_0 B/2m = n_B \qquad 0 \le r \le a \tag{16}$$

where n_B is known as the Brillouin density.

As more electrons are injected the total number of the trapped electrons increases

$$N = \pi a^2 n L \tag{17}$$

where L is the axial length of the plasma. Since the density is always at the Brillouin limit, the plasma radius expands as N increases. The plasma potential on the axis Φ_0 deepens accordingly

$$\Phi_0 = -eN(1 + 2ln\,(b/a))/4\pi\varepsilon_0 L \tag{18}$$

If the electron temperature is not negligibly small compared to the confining potential well depth, the electrons at Maxwellian tail can escape from the trap. The flux Γ and the thermal energy flux Q of the escaping electrons are given by

$$\Gamma = 4\pi \int_0^a r dr \int_{v_z = v_1}^{\infty} f v_z dv^3 \tag{19}$$

$$Q = 4\pi \int_0^a r dr \int_{v_z = v_1}^{\infty} f v_z (\vec{v} - \omega r\vec{\theta})^2 (m/2) dv^3 \tag{20}$$

where $v_I^2 = 2(-eV^* + e\Phi)/m$ and V* is the shallower of the trapping voltages; either on the cathode or the electrode at the opposite end. It must satisfy

$$-V - \phi < -V^* < -V \tag{21}$$

It is preferred that the electrons escape toward the end opposite to the cathode in the experiments because the escaping flux can be measured separately. We obtain

$$\Gamma = (2kT_e/\pi m)^{1/2}(N/L)\gamma^{-1}\{1 - exp(-\gamma)\}exp\{(eV^* - e\Phi_0)/kT_e\} \tag{22}$$

$$Q = \Gamma[kT_e\{2 + (1 - (1+\gamma)e^{-\gamma})(1 - e^{-\gamma})^{-1}\} - eV^* + e\Phi_0] \tag{23}$$

where $\gamma = m\Omega^2 a^2/8kT_e = a^2/4\lambda_D^2$. The factor γ is the manifestation of the fact that the potential well is deeper at the larger radius and the loss is concentrated near the axis.

After the equilibrium given by eq (16) is established, $\gamma >> 1$ and we obtain

$$\Gamma = (2kT_e/\pi m)^{1/2}(4\pi\varepsilon_0 e^{-2})kT_e exp\{e(V^* - \Phi_0)/kT_e\} \tag{24}$$

$$Q = \Gamma[2kT_e - eV^* + e\Phi_0] \tag{25}$$

4. Filling The Trap

The cathode is required to fill the trap in a realistic time. Like any phenomena involving the tunneling the key question is the time scale. In the absence of the plasma loss, the number of the trapped electrons increases as

$$\partial N / \partial t = I / e \tag{26}$$

As the plasma potential builds up, the electric field at the cathode surface and hence the current decrease. We assume that the equilibrium described in the previous section is established soon

after the start of the injection and obtain

$$\frac{\partial E}{\partial t} = -\frac{e(1 + 2ln\ b/a)}{(4\pi\varepsilon_0 RL)} \frac{\partial N}{\partial t} \tag{27}$$

The combination of eq (6), eq (26) and eq (27) yields

$$\frac{\partial E}{\partial t} = -\frac{\alpha R(1 + 2ln\ b/a)}{(4\pi\varepsilon_0 L)} E^2 exp\left(-\frac{\beta}{E}\right) \tag{28}$$

By integration we obtain

$$t = \left(\frac{4\pi\varepsilon_0 L}{\alpha\beta R}\right)(1 + 2ln\ b/a)^{-1}\left\{exp\left(-\frac{\beta}{E}\right) - exp\left(-\frac{\beta}{E_0}\right)\right\} \tag{29}$$

where $E_0 = -V / R$ and V'>> ϕ is assumed.

The following table shows an example of the time dependence of E.

E [10^9v/m]	1.0	1.5	1.75	2.0	2.5	3.0	4.0
t[sec] R[nm]	4.8 x 10^7	1.4 x 10^4	130	3.2	1.8 x 10^{-2}	8.2 x 10^{-6}	6.3 x 10^{-7}

with L =10^{-2} m, ϕ = 4 volt and b/a=1000.

The electric field E* below which the time scale becomes extremely long is roughly given by

$$E^* = 2.5 \times 10^8 \phi^{3/2} \tag{30}$$

and the corresponding plasma potential is given by

$$\Phi_0 = V + \phi R/R^* \tag{31}$$

where $R^* = 4.0 \times 10^{-9}\phi^{-1/2}$.

If the cathode tip is very sharp and R < R* is satisfied. the revised formula for the current given by eq (7) must be used. In this case the filling time becomes very long when

$$\Phi_0 = V + \phi + \Delta\phi \tag{32}$$

The value of $\Delta\phi$ depends somewhat on R and is typically $\phi/2$.

For a fixed cathode voltage, the plasma potential can reach the value given either by eq (31) or eq (32). The number of the trapped electrons which is proportional to the plasma potential can be increased by increasing the cathode voltage.

5. Evaporative Cooling

The injected electrons thermalize through the electron-electron collisions. The collision frequency ν_{ee} at the Brillouin density is given by

$$\nu_{ee} = 1.4 \times 10^8 (kT_e/e)^{-3/2} B^2 \tag{33}$$

and the thermalization proceed rapidly. The electrons at Maxwellian tail have enough energies to escape from the trap. The time evolution of the equilibrium is described by

$$\partial N/\partial t = I/e - \Gamma \tag{34}$$

When the particle balance is maintained, i.e.

$$I = e\Gamma \tag{35}$$

the electron temperature varies as

$$\frac{3}{2}N\frac{\partial kT_e}{\partial t} = -\Gamma\left[eV + e\phi - eV^* + 2k(T_e - T)\right] \tag{36}$$

The right hand side represents the evaporative cooling.

Ordinarily the steady states [$\partial N/\partial t = \partial T_e/\partial t = 0$] are calculated and the accessibility of the steady state can be discussed. However in this case both the field emission current and the evaporation rate contain the exponential factors which act almost as an on-off switch. Therefore the experimental steady state to be defined as the state both the injection and the evaporation are turned off.

We define "steady state" by

$$I < I_{min} \tag{37}$$

$$e\Gamma < I_{min} \tag{38}$$

where I_{min} is chosen depending on the time scale of the experiment. For example, if the experimental confinement time is τ_m, one may choose $I_{min} = eN/10\tau_m$.

The condition (37) has already been discussed in the previous section. For a given cathode voltage when the plasma potential reaches the value given by either eq (31) or eq (32) depending on $R \lesseqgtr R^*$, the injection practically ceases. If the cathode voltage is increased further the injection resumes and more electrons are trapped before the condition (37) is met again. On the other hand if the cathode voltage is reduced the injection current remains off. Thus the region

$$V < \Phi_0 < V + \phi + \Delta\phi \tag{39}$$

can be accessed only by reducing the cathode voltage after the condition (37) is reached.

The evaporation steady state is reached when

$$\left(\frac{2e}{\pi m}\right)^{1/2} 4\pi\varepsilon_0 \left(\frac{kT_e}{e}\right)^{3/2} exp\left[-e(-V^* + \Phi)/kT_e\right] < I_{min} \tag{40}$$

The above condition determines the lowest electron temperature reachable. When the injection

and the evaporation are operating simultaneously, the value of - V* + Φ cannot be smaller than Δϕ. Therefore accessible electron temperature is a fraction, typically 1/20 of eϕ. By reducing the cathode voltage and turning off the injection, the plasma potential can be brought in the range given by eq (39). The value of - V*+ Φ can be as small as one wishes and very low electron temperatures become accessible. We shall examine this case.

In the absence of the injection we obtain

$$\partial N/\partial t = - C(kT_e/e)^{3/2} exp\,(-\xi) \tag{41}$$

$$(3/2)\partial NkT_e/\partial t = - C(kT_e/e)^{3/2} kT_e(2 + \xi) exp\,(-\xi) \tag{42}$$

where $C = (2e/\pi m)^{1/2} 4\pi\varepsilon_0 / e$ and $\xi = e(- V^* + \Phi)/kT_e$. The combination of the above equations yields

$$(1/kT_e)\partial kT_e/\partial t = N^{-1}(\partial N/\partial t)(1 + 2\xi)/3 \tag{43}$$

When $\xi >> 1$, the cooling rate is much faster than the loss rate of the electrons. We construct a simple analytical solution by stipulating that V* is controlled in such a way to keep ξ time independent. The solutions are

$$N = N_0\left(1 + \frac{t}{\tau}\right)^{-\frac{2}{2\xi - 1}} \tag{44}$$

$$T_e = T_{e0}\left(1 + \frac{t}{\tau}\right)^{-\frac{2}{3}\frac{2\xi + 1}{2\xi - 1}} \tag{45}$$

where $\tau = \{2/(2\xi - 1)\}(N_0/C)(kT_{e0}/e)^{-3/2} exp\,(\xi)$ and the subscript 0 denotes the values at t=0. To keep ξ time independent V* should be varied as

$$- V^* = \xi\left(\frac{kT_{e0}}{e}\right)\left(1 + \frac{t}{\tau}\right)^{-\frac{2}{3}\frac{2\xi + 1}{2\xi - 1}} - \Phi_{00}\left(1 + \frac{t}{\tau}\right)^{-\frac{2}{2\xi - 1}} \tag{46}$$

For large values of ξ the change in N is small compared to the change in the temperature.

$$T_e/T_{e0} = (N/N_0)^{(2\xi+1)/3} \tag{47}$$

For example the reduction of the temperature by factor 1000 is accomplished by the reduction of the number of the trapped electrons by factor of 2.7 with $\xi = 10$.

The time scale for the electron temperature to decrease is

$$\frac{T_e}{T_{e0}} \sim \left(\frac{1}{\tau}\right)^{-\frac{2}{3}\frac{2\xi+1}{2\xi-1}} \tag{48}$$

For $\xi = 5$ and $T_e/T_{eo} \sim 1000$ the time is $4.8 \times 10^3\tau$. If N_o is 10^7 and $kT_{e0} = 0.1eV$, τ is 4.0×10^{-5} sec and the time to reach 10^{-4} eV is 0.19sec. The number of the trapped electrons is reduced to 15% of the initial number.

6. Collisional Heating and Field Error Loss

The electrons are heated by the collisions with the residual gas atoms or molecules because the rotational velocity ωr is much larger than the thermal velocity.

The heating rate Q^+ is given by

$$Q^+ = 2\pi\int_0^a r\,dr(nm\omega^2 r^2 \nu_{e0}/2) \tag{49}$$

where ν_{e0} is the electron neutral collision frequency. The cross-section for the electron-neutral collisions is proportional to the reciprocal of the electron velocity and the collision frequency is given by

$$\nu_{e0} = (\pi e^2 a_0^3 \alpha_r)^{1/2} n_0 \tag{50}$$

where a_0 is the Bohr radius, α_r is the relative polarizability of the gas molecules and n_0 is the gas

number density. Typical values of α_r are 10.6 for O_2 and 11 for Ar.

By integration we obtain

$$Q^+ = (\pi e^2 a_0^3 \alpha_r / \varepsilon_0 m)^{1/2} e^2 N^2 n_0 / 8\pi\varepsilon_0 L \qquad (51)$$
$$= 1.45 \times 10^{-41} N^2 n_0 / L$$

We add the heating term to eq (42) and obtain

$$(3/2) N \partial k T_e / \partial t = -\Gamma k T_e (2 + \xi) + Q^+ \qquad (52)$$

The balance between the evaporative cooling and the collisional heating occurs at

$$eC(kT_e/e)^{5/2}(2 + \xi) exp(-\xi) = (\pi e^2 a_0^3 \alpha_n / \varepsilon_0 m)^{1/2} e^2 N^2 n_0 / 8\pi\varepsilon_0 L \qquad (53)$$

or numerically

$$(kT_e/e)^{5/2}(2 + \xi) exp(-\xi) = 3.5 \times 10^{-37} N^2 n_0 / L$$

The above formula gives the lowest temperature achievable for a given residual gas pressure. For example with $\xi = 10$, L= 10^{-2} m and N= 10^6 the residual gas pressure must be below 8.5 x 10^{-10} torr. For larger numbers of the trapped electrons the required residual gas pressure scales as the reciprocal of the square of the number. It is because the rotational kinetic energy increases as the square of the number of the electrons.

In the experiments the axi-symmetry of the trap is not perfect. It has been observed that the plasma slowly expands and is lost even in very high vacuum. The cause of the loss is attributed the field errors which make the system slightly non-symmetric. The confinement time was found to scale as $[B/L]^2$. The best result so far is given by [4]

$$\tau_m [sec] = 3.2 \times 10^3 (B[T] / L[m])^2 \qquad (54)$$

where τ_m is the experimental confinement time. The confinement is also affected by the residual gas pressure. The experimental scaling is given by

$$\tau_g\,[sec] = 2.8 \times 10^{-4} B[T]^2 / p_0[torr] \qquad (55)$$

where τ_g is the confinement time when the effect of the residual gas dominates and p_o is the pressure of the residual gas. The critical pressure below which the effect of the field error dominates is given by

$$p_0[torr] < 8.8 \times 10^{-8} L[m]^2 \qquad (56)$$

For L= 10^{-2}m, the field error effect dominates below pressure of about 10^{-11} torr.

Both the field error and the collisions with the residual gas causes the plasma loss by imparting the drag force on the rotational motion of the plasma. Since the electron heating is also caused by the drag, it may be conjectured that the similar scaling holds for the electron heating.

7. Plasma regimes

The field emission cathode can produce electron plasmas at the Brillouin density because the electrons are injected with zero canonical angular momentum. The electron can be cooled by the evaporative cooling or other means such as the radiative cooling. There are three distinctive regimes depending on the electron temperature.

A] Classical electron plasma

This regime is most readily obtained. The condition that the Debye length is much smaller than the plasma radius is given by

$$kT_e/e << 5.8 \times 10^{-7} N \qquad (57)$$

The evaporative cooling concurrent with the injection will cool the electrons to a fraction of eV and the trapping of the electrons $N > 10^7$ will satisfy the above condition.

B] Strongly correlated electron plasma

The condition that the electrons are strongly correlated is given by

$$n\lambda_D << 1 \tag{58}$$

By using $n = n_B$, the condition becomes

$$T_e[°K] << 3.6 \times 10^2 B[T]^{2/3} \tag{59}$$

The evaporative cooling after the emission is turned of is required to reach this regime.

C] Quantum mechanical electron plasma

This regime requires

$$kT_e < \hbar\Omega/2 \tag{60}$$
$$T_e[°K] < 0.63\, B[T]$$

Intensive cooling, high vacuum and strong magnetic field are needed to enter this regime.

In summary, the electron trap filled by the field emission cathode is proposed. The energy of the electrons tunneling out of metal is lower than the cathode voltage and the static trapping is possible. The injection on the cylindrical axis ensures that the canonical angular momentum of the electrons vanishes. Thus the density at the Brillouin limit is readily obtained. It may be possible to achieve the strongly correlated plasma and even the quantum mechanical plasma regimes with the evaporative cooling.

8. Acknowledgement

The author wishes to thank the non-neutral plasma group at UCSD lead by Profs. T. O'Neil, D. Rubin and F. Driscoll for stimulating discussions.

9. References

[1] R.H. Fowler and L.W. Nordheim, *Proc. Roy. Soc.* **A 119** 173 (1928)

[2] C.A. Spindt, *J. Appl. Phys.* **39** 3504 (1968)

[3] T.M. O'Neil, *Nonneutral plasma physics AIP* 6 (1988)

[4] C.F. Driscoll and J.H. Malmberg, *Phys. Rev. Let.* **50** 167 (1983)

[5] C.F. Driscoll, K.S. Fine and J.H.Malmberg, *Phys. Fluid* **29** 2015 (1986)

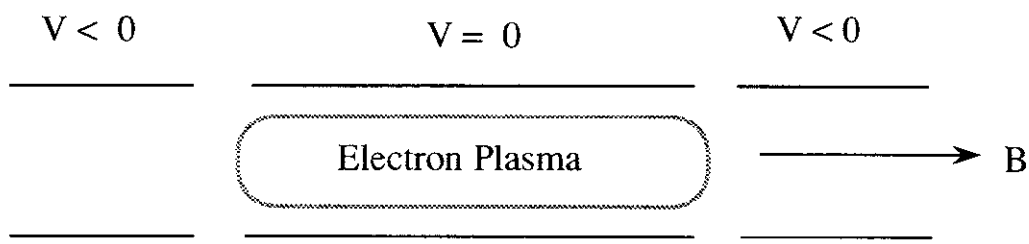

Fig. 1

Penning - Malmberg Trap

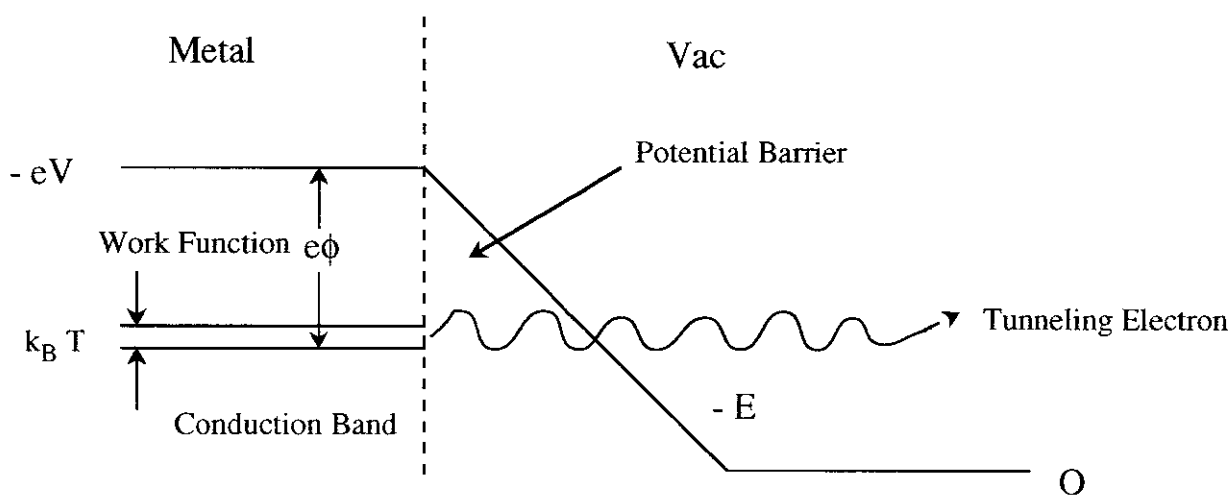

Fig. 2

Energy Diagram of Electrons

Recent Issues of NIFS Series

NIFS-476 Y. Takeiri, M. Osakabe, Y. Oka, K. Tsumori, O. Kaneko, T. Takanashi, E. Asano, T. Kawamoto, R. Akiyama and T. Kuroda,
Long-pulse Operation of a Cesium-Seeded High-Current Large Negative Ion Source; Jan. 1997

NIFS-477 H. Kuramoto, K. Toi, N. Haraki, K. Sato, J. Xu, A. Ejiri, K. Narihara, T. Seki, S. Ohdachi, K. Adati, R. Akiyama, Y. Hamada, S. Hirokura, K. Kawahata and M. Kojima,
Study of Toroidal Current Penetration during Current Ramp in JIPP T-IIU with Fast Response Zeeman Polarimeter; Jan., 1997

NIFS-478 H. Sugama and W. Horton,
Neoclassical Electron and Ion Transport in Toroidally Rotating Plasmas; Jan. 1997

NIFS-479 V.L. Vdovin and I.V. Kamenskij,
3D Electromagnetic Theory of ICRF Multi Port Multi Loop Antenna; Jan. 1997

NIFS-480 W.X. Wang, M. Okamoto, N. Nakajima, S Murakami and N. Ohyabu,
Cooling Effect of Secondary Electrons in the High Temperature Divertor Operation; Feb. 1997

NIFS-481 K. Itoh, S.-I. Itoh, H. Soltwisch and H.R. Koslowski,
Generation of Toroidal Current Sheet at Sawtooth Crash; Feb. 1997

NIFS-482 K. Ichiguchi,
Collisionality Dependence of Mercier Stability in LHD Equilibria with Bootstrap Currents; Feb. 1997

NIFS-483 S. Fujiwara and T. Sato,
Molecular Dynamics Simulations of Structural Formation of a Single Polymer Chain: Bond-orientational Order and Conformational Defects; Feb. 1997

NIFS-484 T. Ohkawa,
Reduction of Turbulence by Sheared Toroidal Flow on a Flux Surface; Feb. 1997

NIFS-485 K. Narihara, K. Toi, Y. Hamada, K. Yamauchi, K. Adachi, I. Yamada, K. N. Sato, K. Kawahata, A. Nishizawa, S. Ohdachi, K. Sato, T. Seki, T. Watari, J. Xu, A. Ejiri, S. Hirokura, K. Ida, Y. Kawasumi, M. Kojima, H. Sakakita, T. Ido, K. Kitachi, J. Koog and H. Kuramoto,
Observation of Dusts by Laser Scattering Method in theJIPPT-IIU Tokamak Mar. 1997

NIFS-486 S. Bazdenkov, T. Sato and The Complexity Simulation Group,
Topological Transformations in Isolated Straight Magnetic Flux Tube; Mar. 1997

NIFS-487 M. Okamoto,
Configuration Studies of LHD Plasmas; Mar. 1997

NIFS-488 A. Fujisawa, H. Iguchi, H. Sanuki, K. Itoh, S. Lee, Y. Hamada, S. Kubo, H. Idei, R. Akiyama, K. Tanaka, T. Minami, K. Ida, S. Nishimura, S. Morita, M. Kojima, S. Hidekuma, S.-I. Itoh, C. Takahashi, N. Inoue, H. Suzuki, S. Okamura and K. Matsuoka,
Dynamic Behavior of Potential in the Plasma Core of the CHS Heliotron/Torsatron; Apr. 1997

NIFS-489 T. Ohkawa,
Pfirsch - Schlüter Diffusion with Anisotropic and Nonuniform Superthermal Ion Pressure; Apr. 1997

NIFS-490 S. Ishiguro and The Complexity Simulation Group,
Formation of Wave-front Pattern Accompanied by Current-driven Electrostatic Ion-cyclotron Instabilities; Apr. 1997

NIFS-491 A. Ejiri, K. Shinohara and K. Kawahata,
An Algorithm to Remove Fringe Jumps and its Application to Microwave Reflectometry; Apr. 1997

NIFS-492 K. Ichiguchi, N. Nakajima, M. Okamoto,
Bootstrap Current in the Large Helical Device with Unbalanced Helical Coil Currents; Apr. 1997

NIFS-493 S. Ishiguro, T. Sato, H. Takamaru and The Complexity Simulation Group,
V-shaped dc Potential Structure Caused by Current-driven Electrostatic Ion-cyclotron Instability; May 1997

NIFS-494 K. Nishimura, R. Horiuchi, T. Sato,
Tilt Stabilization by Energetic Ions Crossing Magnetic Separatrix in Field-Reversed Configuration; June 1997

NIFS-495 T. -H. Watanabe and T. Sato,
Magnetohydrodynamic Approach to the Feedback Instability; July 1997

NIFS-496 K. Itoh, T. Ohkawa, S. -I.Itoh, M. Yagi and A. Fukuyama
Suppression of Plasma Turbulence by Asymmetric Superthermal Ions; July 1997

NIFS-497 T. Takahashi, Y. Tomita, H. Momota and Nikita V. Shabrov,
Collisionless Pitch Angle Scattering of Plasma Ions at the Edge Region of an FRC; July 1997

NIFS-498 M. Tanaka, A.Yu Grosberg, V.S. Pande and T. Tanaka,
Molecular Dynamics and Structure Organization in Strongly-Coupled Chain of Charged Particles; July 1997

NIFS-499 S. Goto and S. Kida,

Direct-interaction Approximation and Reynolds-number Reversed Expansion for a Dynamical System; July 1997

NIFS-500 K. Tsuzuki, N. Inoue, A. Sagara, N. Noda, O. Motojima, T. Mochizuki, T. Hino and T. Yamashina,
Dynamic Behavior of Hydrogen Atoms with a Boronized Wall; July 1997

NIFS-501 I. Viniar and S. Sudo,
Multibarrel Repetitive Injector with a Porous Pellet Formation Unit; July 1997

NIFS-502 V. Vdovin, T. Watari and A. Fukuyama,
An Option of ICRF Ion Heating Scenario in Large Helical Device; July 1997

NIFS-503 E. Segre and S. Kida,
Late States of Incompressible 2D Decaying Vorticity Fields; Aug. 1997

NIFS-504 S. Fujiwara and T. Sato,
Molecular Dynamics Simulation of Structural Formation of Short Polymer Chains; Aug. 1997

NIFS-505 S. Bazdenkov and T. Sato
Low-Dimensional Model of Resistive Interchange Convection in Magnetized Plasmas; Sep. 1997

NIFS-506 H. Kitauchi and S. Kida,
Intensification of Magnetic Field by Concentrate-and-Stretch of Magnetic Flux Lines; Sep. 1997

NIFS-507 R.L. Dewar,
Reduced form of MHD Lagrangian for Ballooning Modes; Sep. 1997

NIFS-508 Y.-N. Nejoh,
Dynamics of the Dust Charging on Electrostatic Waves in a Dusty Plasma with Trapped Electrons; Sep.1997

NIFS-509 E. Matsunaga, T.Yabe and M. Tajima,
Baroclinic Vortex Generation by a Comet Shoemaker-Levy 9 Impact; Sep. 1997

NIFS-510 C.C. Hegna and N. Nakajima,
On the Stability of Mercier and Ballooning Modes in Stellarator Configurations; Oct. 1997

NIFS-511 K. Orito and T. Hatori,
Rotation and Oscillation of Nonlinear Dipole Vortex in the Drift-Unstable Plasma; Oct. 1997

NIFS-512 J. Uramoto,

Clear Detection of Negative Pionlike Particles from H_2 Gas Discharge in Magnetic Field; Oct. 1997

NIFS-513 T. Shimozuma, M. Sato, Y. Takita, S. Ito, S. Kubo, H. Idei, K. Ohkubo, T. Watari, T.S. Chu, K. Felch, P. Cahalan and C.M. Loring, Jr,
The First Preliminary Experiments on an 84 GHz Gyrotron with a Single-Stage Depressed Collector; Oct. 1997

NIFS-514 T. Shjmozuma, S. Morimoto, M. Sato. Y. Takita, S. Ito, S. Kubo, H. Idei, K. Ohkubo and T. Watari,
A Forced Gas-Cooled Single-Disk Window Using Silicon Nitride Composite for High Power CW Millimeter Waves; Oct. 1997

NIFS-515 K. Akaishi,
On the Solution of the Outgassing Equation for the Pump-down of an Unbaked Vacuum System; Oct. 1997

NIFS-516 *Papers Presented at the 6th H-mode Workshop (Seeon, Germany)*; Oct. 1997

NIFS-517 John L. Johnson,
The Quest for Fusion Energy; Oct. 1997

NIFS-518 J. Chen, N. Nakajima and M. Okamoto,
Shift-and-Inverse Lanczos Algorithm for Ideal MHD Stability Analysis; Nov. 1997

NIFS-519 M. Yokoyama, N. Nakajima and M. Okamoto,
Nonlinear Incompressible Poloidal Viscosity in L=2 Heliotron and Quasi-Symmetric Stellarators; Nov. 1997

NIFS-520 S. Kida and H. Miura,
Identificaiton and Analysis of Vortical Structures; Nov. 1997

NIFS-521 K. Ida, S. Nishimura, T. Minami, K. Tanaka, S. Okamura, M. Osakabe, H. Idei, S. Kubo, C. Takahashi and K. Matsuoka,
High Ion Temperature Mode in CHS Heliotron/torsatron Plasmas; Nov. 1997

NIFS-522 M. Yokoyama, N. Nakajima and M. Okamoto,
Realization and Classification of Symmetric Stellarator Configurations through Plasma Boundary Modulations; Dec. 1997

NIFS-523 H. Kitauchi,
Topological Structure of Magnetic Flux Lines Generated by Thermal Convection in a Rotating Spherical Shell; Dec. 1997

NIFS-524 T. Ohkawa,
Tunneling Electron Trap; Dec. 1997